Phytochemistry Letters 43 (2021) 98–102

Contents lists available at ScienceDirect

Phytochemistry Letters

journal homepage: www.elsevier.com/locate/phytol

Three sesquiterpenes from the marine-alga-epiphytic fungus *Trichoderma hamatum* Z36-7

Xin-Yue Ma [a,b], Yin-Ping Song [a], Zhen-Zhen Shi [a,*], Nai-Yun Ji [a,*]

[a] Yantai Institute of Coastal Zone Research, Center for Ocean Mega-Science, Chinese Academy of Sciences, Yantai, 264003, People's Republic of China
[b] University of Chinese Academy of Sciences, Beijing, 100049, People's Republic of China

ARTICLE INFO

Keywords:
Trichoderma hamatum
Terpene
Sesquiterpene
Cyclonerane
Trichothecane

ABSTRACT

Two new cyclonerane sesquiterpenes, 5-hydroxyepicyclonerodiol oxide (**1**) and 4-hydroxyepicyclonerodiol oxide (**2**), and one new naturally occurring halogenated trichothecane derivative, trichodermol chlorohydrin (**3**), were isolated from *Trichoderma hamatum* Z36−7, an epiphytic fungal strain obtained from the marine red alga *Grateloupia* sp. Their structures and relative configurations were assigned on the basis of spectroscopic techniques, including 1D/2D NMR and IR as well as MS. Compound **2** features an unusual 4-hydroxy group on the five-membered ring of cycloneranes, and **3** is the first natural isolate of halogenated trichothecanes. These isolates represent the first occurrence of terpenes in *T. hamatum* and exhibit growth inhibition of several bacteria and phytoplankton species.

1. Introduction

Sesquiterpenes are almost ubiquitous in *Trichoderma* species, such as *T. asperellum* (Shi et al., 2019; Song et al., 2019), *T. brevicompactum* (Klaiklay et al., 2019; Shi et al., 2020), *T. citrinoviride* (Liu et al., 2020), *T. harzianum* (Song et al., 2018), *T. polysporum* (Fujita et al., 1984), and *T. virens* (Song et al., 2020), and they contain at least ten kinds of frameworks (Reino et al., 2008). Although *T. hamatum* has proven to produce a series of simple isonitrile (isocyanide) and cyclopentanone derivatives as well as a pentacyclic polyketide (Baldwin et al., 1985; Boyd et al., 1991; Brewer et al., 1979; Matsumoto et al., 1999; Sakuno et al., 2000), no sesquiterpenes and other terpenes have previously been discovered from this species. During our continuing investigation toward the structural diversity of secondary metabolites from marine-derived *Trichoderma* (Liu et al., 2020; Shi et al., 2020; Song et al., 2020), an epiphytic isolate *Trichoderma hamatum* Z36-7 obtained from the marine red alga *Grateloupia* sp. was chemically examined. Our efforts led to the isolation and identification of two new cyclonerane derivatives (**1** and **2**) and one new naturally occurring trichothecane derivative (**3**) (Fig. 1). Details of isolation, structure elucidation, and bioactivity of these compounds are described in the present paper.

2. Results and discussion

Compound **1** was purified as a colorless oil. Its molecular formula was established as $C_{15}H_{28}O_4$, implying two degrees of unsaturation, by analysis of HRESIMS data (*m/z* 295.1895 $[M+Na]^+$). The IR absorption band at 3420 cm^{-1} indicated the presence of hydroxy groups. Aided by HSQC data, the ^1H NMR spectrum (Table 1) showed notable signals including one doublet of double doublets and one multiplet attributable to two oxymethines, four methyl singlets, and one methyl doublet. Combined with DEPT data, the ^{13}C NMR spectrum (Table 2) demonstrated the presence of five methyls, three methylenes, four methines including two oxymethines at δ_C 74.6 and 86.8, and three oxygenated nonprotonated carbons. The NMR data of **1** were similar to those reported for epicyclonerodiol oxide (Fujita et al., 1984), except for the presence of signals for an oxymethine group and the absence of signals for a methylene group. This oxymethine group was located at C-5 based on the COSY correlations from H-2 to H_3-1 and H-6 and from H-5 to H_2-4 and H-6. Thus, compound **1** was deduced to be 5-hydroxyepicyclonerodiol oxide. Its structure was further confirmed by the COSY correlations from H_2-9 to H_2-8 and H-10 and by the HMBC correlations from H_3-1 to C-2, C-3, and C-6, from H_3-12 to C-10, C-11, and C-15, from H_3-13 to C-2, C-3, and C-4, from H_3-14 to C-6, C-7, and C-8, and from H_3-15 to C-10, C-11, and C-12 (Fig. 1). The NOE correlation between H_3-1 and H-6 indicated C-1 and H-6 to be on the same face of ring A, while

* Corresponding authors.
E-mail addresses: zzshi@yic.ac.cn (Z.-Z. Shi), nyji@yic.ac.cn (N.-Y. Ji).

https://doi.org/10.1016/j.phytol.2021.03.020
Received 14 January 2021; Received in revised form 8 March 2021; Accepted 24 March 2021
Available online 2 April 2021

correlations from H-2 to H_3-13 and from H-5 to H_3-14 located H-2, H-5, C-7, and C-13 on the other face (Fig. 2). Additionally, the relative configuration around ring B was proposed to be the same as that of epicyclonerodiol oxide based on the identical NMR data (Fujita et al., 1984).

Compound **2** was obtained as a colorless oil. HRESIMS (*m/z* 295.1888 $[M + Na]^+$) analysis gave the molecular formula of $C_{15}H_{28}O_4$, the same as for **1**. The IR spectrum displayed a broad absorption band at 3428 cm^{-1}, corresponding to the presence of hydroxy groups. Its ^1H and ^{13}C NMR spectra (Tables 1 and 2) also exhibited the signals for five methyls, three methylenes, four methines including two oxygen-bearing ones, and three oxygenated nonprotonated carbons. Types and chemical shifts of the above groups were identical with those of **1**, except for the different chemical shifts for a pair of oxymethine groups. The oxymethine group at δ_C 78.3 was located at C-4 on the basis of its HMBC correlations with C-3 and C-13. Thus, compound **2** was proposed to be 4-hydroxyepicyclonerodiol oxide, validated by other COSY and HMBC correlations (Fig. 1). The relative configuration around ring A was confirmed by the NOE correlations from H_3-13 to H-2 and H-4 and from H_3-1 to H-6 (Fig. 2), while that around ring B was deduced to be the same as **1** in view of the identical NMR data.

The positive ESI mass spectrum of compound **3**, obtained as colorless needles, exhibited a characteristic quasimolecular ion peak cluster at *m/*

Table 1
^1H NMR (500 MHz) data for **1**–**3** (in $CDCl_3$).

pos	1	2	3
1	1.07, d (6.8)	1.08, d (6.9)	3.71, d (5.2)
2	1.56, dq (9.8, 6.8)	1.65, dq (8.6, 6.9)	5.51, m
4a	1.85, m	3.73, dd (8.4)	2.03, m
4b	1.85, m	–	1.93, dd (18.2, 5.6)
5a	4.10, ddd (5.0, 3.6, 3.6)	1.76, m	1.72, m
5b	–	1.76, m	1.31, dddd (12.9, 5.6, 1.4, 1.4)
6	1.96, dd (9.8, 3.5)	1.99, ddd (10.6, 8.7, 4.9)	–
8a	1.92, m	1.84, m	4.21, dd (10.0, 5.6)
8b	1.79, m	1.69, m	–
9a	1.92, m	1.85, m	2.43, ddd (11.9, 5.6, 6.0)
9b	1.82, m	1.78, m	2.04, ddd (11.9, 11.3, 10.0)
10	3.72, m	3.69, m	4.14, dd (11.3, 6.0)
12	1.12, s	1.10, s	3.87, br s
13	1.26, s	1.21, s	1.12, s
14	1.20, s	1.16, s	0.90, s
15	1.21, s	1.20, s	1.72, s
OH-12	–	–	2.17, br s

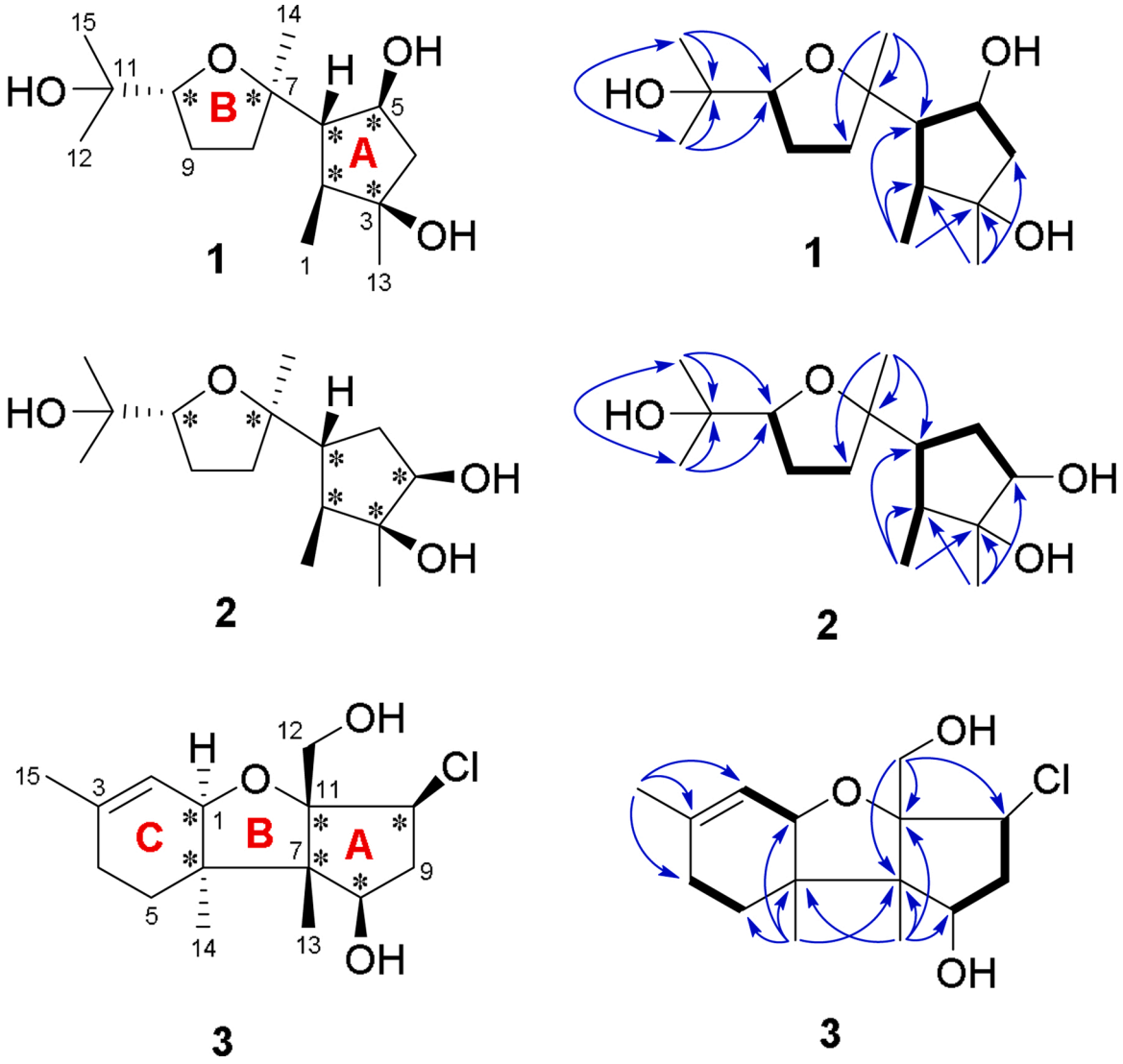

Fig. 1. Structures and Key HMBC (arrows) and COSY (bold lines) correlations of **1**–**3** (* chiral carbon atoms with relative configurations being shown).

Table 2
^{13}C NMR (125 MHz) data for **1**–**3** (in $CDCl_3$).

pos	1	2	3
1	13.5, CH_3	14.4, CH_3	77.9, C
2	45.5, CH	42.5, CH	117.6, CH
3	81.1, C	79.9, C	141.2, C
4	48.7, CH_2	78.3, CH	28.1, CH_2
5	74.6, CH	34.2, CH_2	25.6, CH_2
6	65.2, CH	51.4, CH	43.6, C
7	85.1, C	85.6, C	58.9, C
8	37.1, CH_2	35.5, CH_2	72.4, CH
9	26.4, CH_2	26.3, CH_2	42.0, CH_2
10	86.8, CH	87.2, CH	63.8, CH
11	70.4, C	70.4, C	91.1, C
12	24.3, CH_3	24.2, CH_3	65.0, CH_2
13	25.7, CH_3	23.6, CH_3	9.9, CH_3
14	25.3, CH_3	27.0, CH_3	14.2, CH_3
15	28.0, CH_3	28.0, CH_3	23.6, CH_3

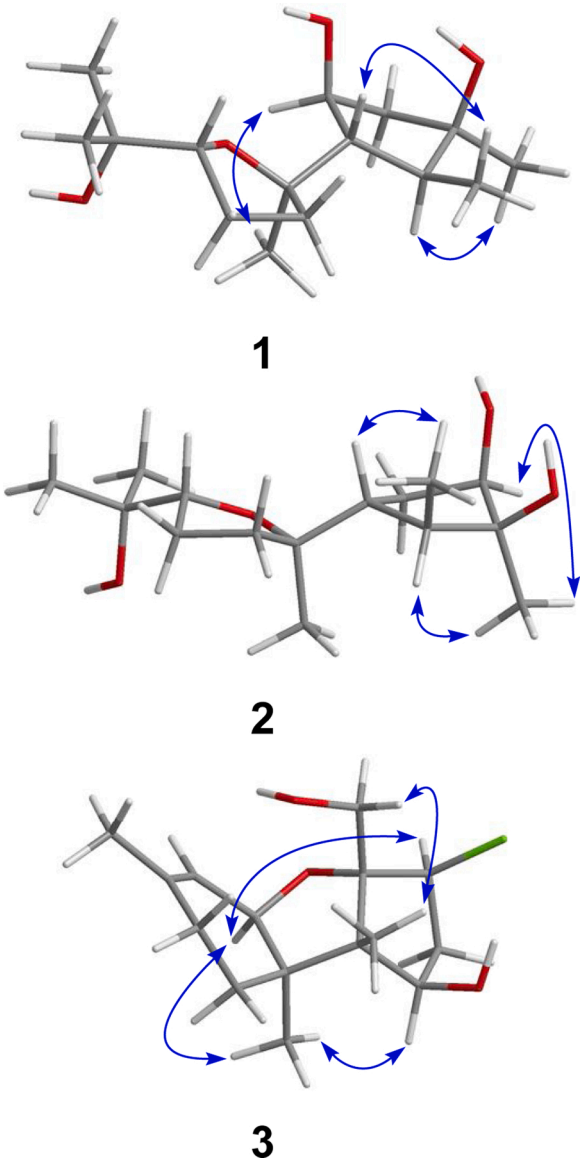

Fig. 2. Key NOE correlations of **1**–**3**.

z 309/311 (3:1) $[M+Na]^+$, suggesting the presence of a chlorine atom. The molecular formula was assigned to be $C_{15}H_{23}ClO_3$, requiring four degrees of unsaturation, by interpretation of HRESIMS data (*m/z* 309.1230 $[M+Na]^+)^{-1}$ in the IR spectrum indicated the presence of hydroxy groups. The ^{1}H NMR chemical shifts (Table 1) at δ_H 5.51 (H-2), 4.14 (H-10), 3.71 (H-1), 1.72 (H_3-15), 1.12 (H_3-13), and 0.90 (H_3-14) resembled those of trichodermol chlorohydrin, an intermediate produced by treatment of trichodermol with hydrochloric acid (Godtfredsen and Vangedal, 1965). However, the deshielded signals at δ_H 4.21 (H-8) and 3.87 (H_2-12) and the shielded signals at δ_H 1.2–2.5 were not reported in the literature. It was arbitrary to judge the identity of **3** based on the limited similarities, therefore the ^{13}C and 2D NMR spectra were further recorded. The signals for three methyls, four methylenes, four methines, and four nonprotonated carbons appeared in the ^{13}C NMR spectrum. These groups were linked together to form a planar structure which was the same as that of trichodermol chlorohydrin indicated by analysis of HMBC correlations (Fig. 1) and by comparison of NMR data with 2,4,12-trihydroxyapotrichothecene (Shi et al., 2020). Thus, compound **3** was identified to be trichodermol chlorohydrin, which was also verified by the identical specific optical rotation and melting point data. The relative configurations at six chiral carbons, which were not fully given in the literature (Godtfredsen and Vangedal, 1965), were confirmed by the NOESY spectrum. In it, the correlations from H-1 to H-10 and H_3-14 oriented H-1, H-10, and C-14 on the same face of rings A, B, and C, while the correlation between H_2-12 and H_3-13 located them on the other face (Fig. 2). Additionally, the NOE correlation between H-8 and H_3-14 suggested not only the cofacial property of H-8 and C-14 but also the opposite relationship of C-13 and C-14.

Compounds **1**–**3** represent the first occurrence of terpenes in *T. hamatum*, but it is regrettable that their absolute configurations have not been determined successfully. It is worth mentioning that **2** is the first member of 4-hydroxy cycloneranes, and **3** is the first natural isolate of halogenated trichothecanes. These compounds greatly add to the structural diversity of secondary metabolites from *T. hamatum*.

The inhibition of marine phytoplankton species by compounds **1**–**3** was assessed with *Amphidinium carterae*, *Chattonella marina*, and *Prorocentrum donghaiense*. As shown in Table 3, all the isolates can inhibit the growth of *C. marina*. Compared to **2** and 10-cycloneren-3,5,7-triol (Song et al., 2018), **1** exhibit a lower effect on *C. marina* and a higher effect on *P. donghaiense*. These differences may correlate to variation (C-4 or C-5) of the hydroxy group and cyclization of the side chain moiety. In addition, the antibacterial activity (Table 3) of these isolates was also assayed against *Vibrio anguillarum*, *V. harveyi*, *V. parahaemolyticus*, and *V. splendidus*. Compounds **1** and **2** can inhibit all the four bacteria, but **3** only shows weak activity against *V. parahaemolyticus*. Although a chlorine atom is present in **3**, it seems unable to improve the antibacterial effect. Overall, none of the isolates exhibit better activities than positive controls.

3. Experimental

3.1. General experimental procedures

The melting point was determined on an SGW X-4 micro-melting-point apparatus (Shanghai Precision & Scientific Instrument Co., Ltd, Shanghai, China). Optical rotations were acquired on an SGW-3 polarimeter (Shanghai Shenguang Instrument Co., Ltd., Shanghai, China). 1D and 2D NMR spectra were measured on a Bruker Avance III 500 NMR spectrometer (500 and 125 MHz for ^{1}H and ^{13}C, respectively) (Bruker Corp., Billerica, MA, USA). IR spectra were recorded on a Nicolet iS50 FT-IR spectrometer (Thermo Fisher Scientific, Waltham, MA, USA). Low- and high-resolution ESI mass spectra were obtained on an Agilent G6230 (Agilent Technologies Inc., Santa Clara, CA, USA) or a Waters ACQUITY TOF mass spectrometer (Waters Corp., Milford, MA, USA). HPLC separation was carried out on an Agilent HPLC system (1260 infinity quaternary pump, 1260 infinity diode-array detector, Agilent Technologies Inc., Santa Clara, CA, USA) with an Eclipse SB-C18 (5 μm, 9.4 ×) column. Column chromatography (CC) was performed with silica gel (200–300 mesh, Qingdao Haiyang Chemical Co., Qingdao, China),

Table 3
Antimicroalgal and antibacterial activities of **1**–**3**.

Compd	IC_{50} (μg/mL)			Inhibitory zone diameter (mm) at 40 μg/disk			
	A. carterae	*C. marina*	*P. donghaiense*	*V. anguillarum*	*V. harveyi*	*V. parahaemolyticus*	*V. splendidus*
1	na	55	35	10	8.5	7.7	7.7
2	na	24	na	9.0	7.7	8.0	6.7
3	97	26	35	0	0	7.0	0
$K_2Cr_2O_7$	1.4	1.1	1.1				
chloramphenicol				30	40	35	40

[na] = no activity at 100 μg/mL.

RP-18 (AAG12S50, YMC Co., Ltd., Kyoto, Japan), and Sephadex LH-20 (GE Healthcare, Uppsala, Sweden). Thin-layer chromatography (TLC) was conducted with precoated silica gel plates (GF-254, Qingdao Haiyang Chemical Co., Qingdao, China).

3.2. Fungal material and fermentation

Trichoderma hamatum Z36-7 was isolated from the surface of the marine red alga *Grateloupia* sp., collected from the coast of Zhoushan Islands in June 2018. The strain was identified by analysis of the morphological characteristics and the ITS sequence that was deposited in GenBank with the accession number MW314739. Its fermentation was carried out statically at room temperature for 45 days in 200 × 1 L Erlenmeyer flasks, each containing 50 g rice, 0.5 g peptone, and 100 mL natural seawater.

3.3. Extraction and isolation

The mycelia were dried, smashed, and then extracted with EtOH. After removing the organic solvent by evaporation under vacuum, the extract (357.4 g) was subjected to silica gel CC with step-gradient solvent systems consisting of petroleum ether (PE)/EtOAc and CH_2Cl_2/MeOH to yield eight fractions (Frs.1–8). Fr. 4 eluted with PE/EtOAc (1:1) and was further purified by RP-18 CC (MeOH/H_2O, 9:1) and preparative TLC (PE/EtOAc, 1:1) as well as semipreparative HPLC (MeOH/H_2O, 3:1 to 6:7, 40 min, 3.0 mL/min, RT =23 min, UV detection at 210 nm) to afford **3** (7.5 mg). Fr. 5 eluted with EtOAc and was further purified by RP-18 CC (MeOH/H_2O, 3:2) and preparative TLC to give **1** (5.7 mg) and **2** (2.5 mg).

3.3.1. 5-Hydroxyepicyclonerodiol oxide (*1*)

Colorless oil; $[\alpha]^{32}_D$ +50 (*c* 0.19, MeOH); IR (KBr) ν_{max} 3420, 2922, 1633, 1384, 1021 cm^{-1}; ^1H and ^{13}C NMR data, Tables 1 and 2; HRESIMS *m/z* 295.1895 $[M + Na]^+$ (calcd for $C_{15}H_{28}O_4Na$, 295.1885).

3.3.2. 4-Hydroxyepicyclonerodiol oxide (*2*)

Colorless oil; $[\alpha]^{33}_D$ +29 (*c* 0.083, MeOH); IR (KBr) ν_{max} 3428, 2967, 2923, 1633, 1384, 1024 cm^{-1}; ^1H and ^{13}C NMR data, Tables 1 and 2; HRESIMS *m/z* 295.1888 $[M + Na]^+$ (calcd for $C_{15}H_{28}O_4Na$, 295.1885).

3.3.3. Trichodermol chlorohydrin (*3*)

Colorless needles; mp 177–179 °C; $[\alpha]^{23}_D$ +7.1 (*c* 0.38, MeOH); IR (KBr) ν_{max} 3444, 2921, 2851, 1633, 1454, 1385, 1262, 995 cm^{-1}; ^1H and ^{13}C NMR data, Tables 1 and 2; ESI(+)MS *m/z* 309, 311 $[M + Na]^+$ (3:1); HRESIMS *m/z* 309.1230 $[M + Na]^+$ (calcd for $C_{15}H_{23}ClO_3Na$, 309.1233).

3.4. Bioassays

Following the previous procedures (Miao et al., 2012; Shi et al., 2018), compounds **1**–**3** were assayed for the inhibition of three marine phytoplankton species (*A. carterae*, *C. marina*, and *P. donghaiense*) and four marine-derived bacteria (*V. anguillarum*, *V. harveyi*, *V. parahaemolyticus*, and *V. splendidus*). $K_2Cr_2O_7$ (purity 99.8 %, Ruijinte Chemical Co., Ltd., Tianjin, China) and chloramphenicol (purity ≥ 99 %, Solarbio Science & Technology Co., Ltd., Beijing, China) were employed as positive controls during the antimicroalgal and antibacterial assays, respectively.

Declaration of Competing Interest

The authors report no declarations of interest.

Acknowledgments

Financial support from the Natural Science Foundation of Shandong Province (ZR2020QD102), the National Natural Science Foundation of China (31670355), and the Taishan Scholar Project Special Funding (tsqn201909164) is gratefully acknowledged.

Appendix A. Supplementary data

Supplementary material related to this article can be found, in the online version, at doi:https://doi.org/10.1016/j.phytol.2021.03.020.

References

Baldwin, J.E., Adlington, R.M., Chondrogianni, J., Edenborough, M.S., Keeping, J.W., Ziegler, C.B., 1985. Structure and synthesis of new cyclopentenyl isonitriles from *Trichoderma hamatum* (Bon.) Bain. aggr. HLX 1379. J. Chem. Soc. Chem. Commun. 816–817.

Boyd, R.K., McAlees, A.J., Taylor, A., Walter, J.A., 1991. Isolation of new isocyanide metabolites of *Trichoderma hamatum* as their (η^5-pentamethylcyclopentadienyl)-or (η^5-ethyltetramethylcyclopentadienyl)-di-μ-thiocyanato-rhodium complexes. J. Chem. Soc. Perkin Trans. 1, 1461–1465.

Brewer, D., Gabe, E.J., Hanson, A.W., Taylor, A., Keeping, J.W., Thaller, V., Das, B.C., 1979. Isonitrile acids from cultures of the fungus *Trichoderma hamatum* (Bon.) Bain. aggr., X-ray structure. J. Chem. Soc. Chem. Commun. 1061–1062.

Fujita, T., Takaishi, Y., Takeda, Y., Fujiyama, T., Nishi, T., 1984. Fungal metabolites. II. Structural elucidation of minor metabolites, valinotricin, cyclonerodiol oxide, and epicyclonerodiol oxide, from *Trichoderma polysporum*. Chem. Pharm. Bull. 32, 4419–4425.

Godtfredsen, W.O., Vangedal, S., 1965. Trichodermin, a new sesquiterpene antibiotic. Acta Chem. Scand. 19, 1088–1102.

Klaiklay, S., Rukachaisirikul, V., Saithong, S., Phongpaichit, S., Sakayaroj, J., 2019. Trichothecenes from a soil-derived *Trichoderma brevicompactum*. J. Nat. Prod. 82, 687–693.

Liu, X.-H., Hou, X.-L., Song, Y.-P., Wang, B.-G., Ji, N.-Y., 2020. Cyclonerane sesquiterpenes and an isocoumarin derivative from the marine-alga-endophytic fungus *Trichoderma citrinoviride* A-WH-20-3. Fitoterapia 141, 104469.

Matsumoto, T., Ishiyama, A., Yamaguchi, Y., Masuma, R., Ui, H., Shiomi, K., Yamada, H., Ōmura, S., 1999. Novel cyclopentanone derivatives pentenocins A and B, with interleukin-1β converting enzyme inhibitory activity, produced by *Trichoderma hamatum* FO-6903. J. Antibiot. 52, 754–757.

Miao, F.-P., Liang, X.-R., Yin, X.-L., Wang, G., Ji, N.-Y., 2012. Absolute configurations of unique harziane diterpenes from *Trichoderma* species. Org. Lett. 14, 3815–3817.

Reino, J.L., Guerrero, R.F., Hernández-Galán, R., Collado, I.G., 2008. Secondary metabolites from species of the biocontrol agent *Trichoderma*. Phytochem. Rev. 7, 89–123.

Sakuno, E., Yabe, K., Hamasaki, T., Nakajima, H., 2000. A new inhibitor of 5'-hydroxyaverantin dehydrogenase, an enzyme involved in aflatoxin biosynthesis, from *Trichoderma hamatum*. J. Nat. Prod. 63, 1677–1678.

Shi, Z.-Z., Miao, F.-P., Fang, S.-T., Yin, X.-L., Ji, N.-Y., 2018. Sulfurated diketopiperazines from an algicolous isolate of *Trichoderma virens*. Phytochem. Lett. 27, 101–104.

Shi, Z.-Z., Miao, F.-P., Fang, S.-T., Yin, X.-L., Ji, N.-Y., 2019. Trichobisabolins A-H, eight new bisabolane derivatives from the marine-alga-epiphytic fungus *Trichoderma asperellum* Y6-2. Fitoterapia 134, 372–377.

Shi, Z.-Z., Liu, X.-H., Li, X.-N., Ji, N.-Y., 2020. Antifungal and antimicroalgal trichothecene sesquiterpenes from the marine algicolous fungus *Trichoderma brevicompactum* A-DL-9-2. J. Agric. Food Chem. 68, 15440–15448.

Song, Y.-P., Fang, S.-T., Miao, F.-P., Yin, X.-L., Ji, N.-Y., 2018. Diterpenes and sesquiterpenes from the marine algicolous fungus *Trichoderma harzianum* X-5. J. Nat. Prod. 81, 2553–2559.

Song, Y.-P., Miao, F.-P., Liang, X.-R., Yin, X.-L., Ji, N.-Y., 2019. Harziane and cadinane terpenoids from the alga-endophytic fungus *Trichoderma asperellum* A-YMD-9-2. Phytochem. Lett. 32, 38–41.

Song, Y.-P., Shi, X.-S., Wang, B.-G., Ji, N.-Y., 2020. Cadinane and carotane derivatives from the marine algicolous fungus *Trichoderma virens* RR-dl-6-8. Fitoterapia 146, 104715.